Magnetization-dependent loss in an (Al,Ga)As optical waveguide with an embedded Fe micromagnet

V. Zayets,* H. Saito, S. Yuasa, and K. Ando

Nanoelectronics Research Institute, National Institute of Advanced Industrial Science and Technology (AIST), Umezono 1-1-4, Tsukuba, Ibaraki 305-8568, Japan
**Corresponding author: v.zayets@aist.go.jp*

Received November 6, 2009; revised January 31, 2010; accepted February 4, 2010; posted February 24, 2010 (Doc. ID 119154); published March 19, 2010

The dependence of waveguiding loss on the magnetization of a Fe micromagnet embedded into the (Al,Ga)As optical waveguide was examined as a possible readout method for the spin-photon memory. The optical detection of the magnetization direction of a Fe micromagnet was demonstrated for the micromagnet sizes of 3 μm$\times$4 μm and 3 μm$\times$8 μm with signal-to-noise ratios of 4.8 and 6 dB, respectively. In the case of smaller sizes, the use of spin injection from the micromagnet into a semiconductor optical amplifier was proposed for the optical detection of the magnetization.

OCIS codes: 210.4680, 210.3810, 230.2240, 320.7085.

High-speed all-optical memory is important for the realization of the next generation of high-speed optical networks [1,2]. The operation speed above 100 Gbits/s and nonvolatile data storing are most desirable features of such a memory. High-speed data processing, chip-to-chip optical connection, and optical buffer memory are a few of the possible applications of a high-speed nonvolatile optical memory. The use of the spin for the optical memory benefits from its ability for the fast operation speed and non-volatile recording. It was demonstrated experimentally that spin polarization in a semiconductor can be switched on and off by the light at a speed as fast as 2.2 Tbits/s [3]. The nonvolatile data recording utilizing spin transfer switching is a current technology of magnetic random assess memory [4].

The design of spin-photon memory was proposed [3]. The memory consists of a micromagnet made of a ferromagnetic metal integrated on a semiconductor photodetector. The size of the micromagnet should be smaller than the domain size of the metal. Then, the micromagnet will be in the single-domain state even without an external magnetic field. The data are stored as a magnetization direction in the micromagnet. The data recording is achieved by reversing the magnetization direction by an optical pulse. The circularly polarized optical pulse is absorbed by the semiconductor photodetector to create spin-polarized electrons. Under an applied voltage these spin-polarized electrons are injected from the detector into the micromagnet. The spin transfer torque is a consequence of the transfer of spin angular momentum from a spin-polarized current to the magnetic moment of a micromagnet. If the torque is sufficient, the magnetization is reversed and the data are memorized. The threshold current for the magnetization reversal is roughly proportional to the volume of the nanomagnet [5,6]. The smaller sizes of the micromagnet, the smaller the threshold current needed for the magnetization reversal and the smaller optical pulse energy required for the recording.

The optical readout is an essential function of a memory. It is possible to detect the magnetization direction utilizing magneto-optical (MO) effect. The required decrease in the sizes of the micromagnet reduces the efficiency of the MO readout. In the case of free-space optics, the resolution of a small object is limited by the diffraction limit given by the Rayleigh criterion. In the case of waveguide there is no such a limit; however it is obvious that the reduction in the size of the micromagnet causes the reduction in the efficiency of the MO readout. Therefore, there is a trade-off between requirements for the smaller size of the micromagnet for the recording and for the larger size of the micromagnet for the readout.

The MO readout can be achieved either by utilizing the Faraday rotation or by the effect of magnetization-dependent loss. In this Letter we studied the effect of magnetization-dependent loss in the AlGaAs optical waveguide with an embedded Fe micromagnet in order to determine the smallest size of the micromagnet when the magnetization can be detected with an acceptable signal-to-noise ratio (SNR).

The magnetization-dependent loss in the semiconductor/metal hybrid waveguide was discovered recently [7] and it was proved experimentally for Co/AlGaAs waveguides [8], MnAs/InGaAsP amplifiers [9], Fe/InGaAsP amplifiers [10], and FeCo/InAlGaAs amplifiers [11]. When one layer of the optical waveguide is a ferromagnetic metal and its magnetization is perpendicular to the mode propagation direction, the optical absorption is different for two opposite directions of the magnetization. Therefore, such a waveguide can function as an optical gate, when the light can be switched on or off by reversing the magnetization of the metal. The magnetization of a ferromagnetic metal can be detected by the intensity of the transmitted light.

The (Al,Ga)As optical waveguide was grown by molecular beam epitaxy. Following a 3-μm-thick $Al_{0.5}Ga_{0.5}As$ clad layer, the 800 nm thick $Al_{0.3}Ga_{0.7}As$

0146-9592/10/070931-3/$15.00

core layer was grown. The 120-nm-deep pit was wet etched through a photoresist mask following the deposition of 40 nm of Fe and 5 nm of Au by sputtering. The metal was lift off. Therefore, the metal remained only inside the pit. The rib waveguide was dry etched with a SiO_2 mask. The height of the rib was 600 nm. The widths of the rib and the Fe micromagnet were the same. The waveguide was covered by 200 nm thick SiO_2 to avoid oxidation. The devices with a variety of lengths and widths of Fe micromagnet were fabricated on the same wafer. The light of the wavelength of 770 nm was coupled in and out of the waveguide using polarization-maintaining fibers. The light intensity was 50–300 μW. The magnetic field was applied perpendicularly to the waveguide and in the film plane. Figure 1(a) shows the structure of the fabricated device. Figure 1(b) shows a scanning-electron-microscope (SEM) cross-section image of the waveguide taken across the waveguide and Fig. 1(c) shows a SEM image taken across the micromagnet. In both cases, the waveguide walls were vertical and the interface between the semiconductor and Fe micromagnet was smooth.

Figure 2 shows the transmission coefficient of the TM waveguide mode as a function of the applied magnetic field for the 3-μm-wide waveguide with the micromagnet lengths of 8 and 4 μm. A clear hysteresis loop for the transmission coefficient was observed in both cases, but the amplitude of the loop was smaller in the case of the shorter micromagnet. The coercive field was 30 Oe in both cases. The loop was not observed in the case of a waveguide without a Fe micromagnet. It proves that the transmission depends on the magnetization direction of the Fe micromagnet. With decreasing of the micromagnet length, both the MO signal and SNR decrease. For a submicrometer-size Fe micromagnet, the MO signal was smaller than the noise level. Figure 3 shows the fiber-to-fiber loss, MO signal, and SNR as functions of the length of the Fe micromagnet. The loss is linearly proportional to the length of the Fe micromagnet as 0.38 dB/μm. The offset loss of 27 dB is due to the fiber-waveguide coupling loss and the scattering loss on the Fe micromagnet. The MO signal is linearly proportional to the micromagnet length for lengths longer than 10 μm. For shorter lengths, the MO signal rapidly decreases. Therefore, in the case when the micromagnet size is comparable with the wavelength, the linear proportionality of the MO signal to the Fe micromagnet length does not hold. The SNR is almost constant around 10 dB for the long lengths, but it rapidly decreases when the micromagnet length becomes comparable with the wavelength of light ($\lambda = 770$ nm).

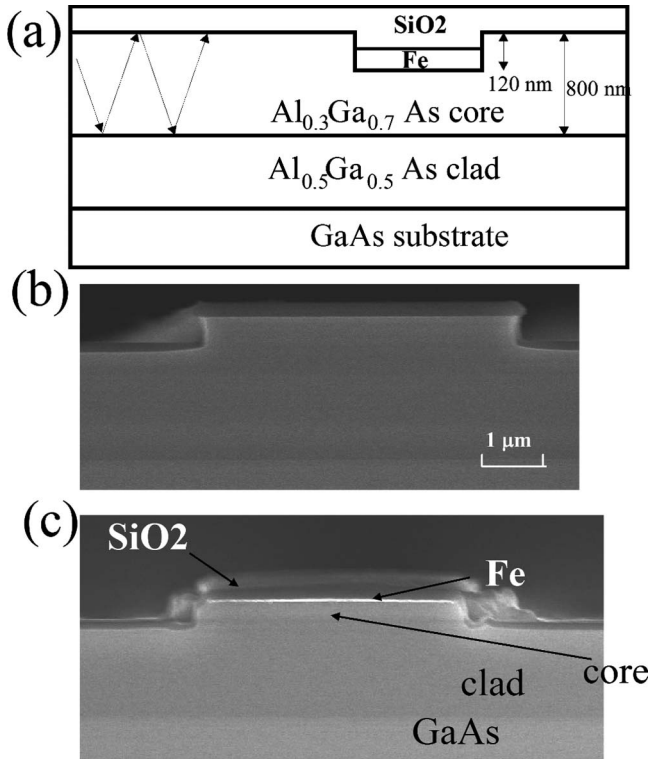

Fig. 1. (a) Structure of (Al,Ga)As waveguide with embedded micromagnet. SEM cross-sectional image taken across the (b) waveguide and (c) micromagnet.

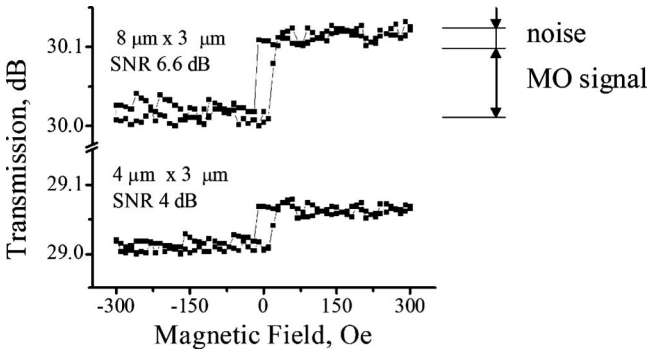

Fig. 2. Transmission of TM mode of rib waveguide with embedded Fe micromagnet as a function of magnetic field applied perpendicularly to the waveguide and in waveguide plane. Micromagnet sizes are 8 μm $\times$ 3 μm and 4 μm $\times$ 3 μm. Amplitude of MO signal and noise were shown.

In the most desirable case, the readout efficiency should not depend on the size of the micromagnet. Therefore, the sizes of the micromagnet could be optimized according to the conditions for the recording. Figure 4 shows a scheme for the proposed solution, which satisfied this condition. The device consists of

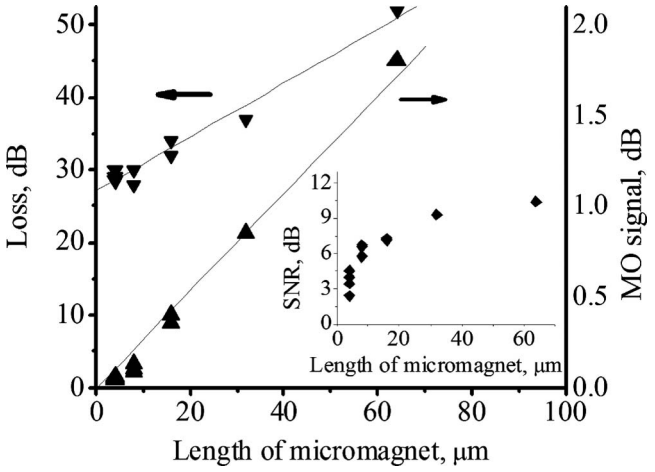

Fig. 3. Fiber-to-fiber loss (inverted triangle), MO signal (triangle), and SNR (inset) as functions of micromagnet length.

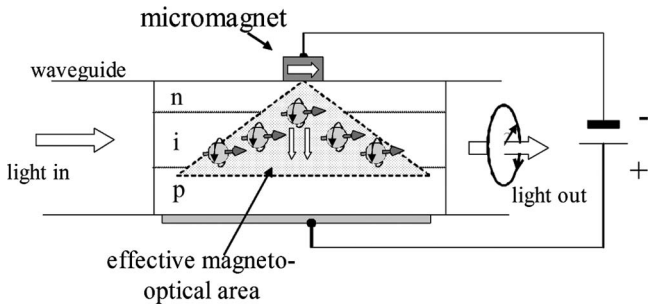

Fig. 4. Proposed design for detection of the magnetization utilizing the spin injection from the micromagnet into p-i-n junction.

a micromagnet fabricated on top of a p-i-n junction. The device structure is the same as it was used for recording [3], except the polarity of the applied voltage between the micromagnet and p-region is reversed. In the case of recording, the spin-polarized electrons are injected from the p-i-n junction into the micromagnet. In the proposed scheme for readout, the spin-polarized electrons are injected from the micromagnet into the p-i-n junction. The input optical pulse of wavelength corresponded to the bandgap of the i-region is used for the readout. Under a forward electrical bias the spin-polarized electrons and unpolarized holes are injected into the i-region of the p-i-n junction and recombines there with the result of stimulated emission and amplification of the input pulse. Owing to the optical selection rule, the amplification for the left and right circular polarizations is different when electrons in the amplifying region are spin-polarized. The polarization of the linearly polarized light will be rotated in this p-i-n junction. The direction of rotation will correspond to the direction of the micromagnet magnetization. Therefore, by detecting the direction of polarization rotation of the output pulse, the data stored in the memory can be read. Owing to the wide spreading of spin-polarized electrons over a larger volume in the p-i-n junction, the effective volume of the MO area will be significantly larger than the volume of the micromagnet. Assuming that the electron spreading has the shape of a rotational semi-ellipsoid [12], the effective MO volume could be as large as 0.1 μm^3, compared with only 10^{-4} μm^3 of the micromagnet volume. Therefore, it could be expected that in this case the MO signal will be significantly greater. Moreover, owing to the optical gain, the MO signal could be further amplified. The spin injection from a ferromagnetic metal into a semiconductor was demonstrated [13], and the difference of electroluminescence between left and right circularly polarized light was observed [14–17]. With an efficient spin injection, the degree of circular polarization can reach up to 32% at room temperature [17]. It proves the feasibility of this method for an effective readout of the magnetization of the submicron-size magnet.

In conclusion, it was demonstrated that the magnetization of a Fe micromagnet embedded into the optical rib waveguide can be detected optically using magnetization-dependent loss in a hybrid ferromagnetic metal/semiconductor waveguide. SNRs of 6.6 and 4 dB were demonstrated for the (Al,Ga)As waveguide with embedded Fe micromagnets with sizes of 3 $\mu m \times 8$ μm and 3 $\mu m \times 4$ μm, respectively. For the smaller micromagnet, the spin injection from the micromagnet into semiconductor was proposed to achieve an efficient readout.

Financial support of the New Energy and Industrial Technology Development Organization (NEDO) is greatly acknowledged. We thank K. Moriyama for technical assistance.

References

1. A. E. F. Burmeister, D. J. Blumenthal, and J. E. Bowers, Opt. Switching Networking **6**, 10 (2008).
2. R. Takahashi, T. Nakahara, K. Takahata, H. Takenouchi, T. Yasui, N. Kondo, and H. Suzuki, IEEE Photon. Technol. Lett. **16**, 1185 (2004).
3. V. Zayets and K. Ando, Appl. Phys. Lett. **94**, 121104 (2009).
4. M. Nakayama, T. Kai, N. Shimomura, M. Amano, E. Kitagawa, T. Nagase, M. Yoshikawa, T. Kishi, S. Ikegawa, and H. Yoda, J. Appl. Phys. **103**, 07A710 (2008).
5. H. Kubota, A. Fukushima, Y. Ootani, S. Yuasa, K. Ando, H. Maehara, K. Tsunekawa, D. D. Djayaprawira, and N. Watanabe, Appl. Phys. Lett. **89**, 032505 (2006).
6. F. J. Albert, N. C. Emley, E. B. Myers, D. C. Ralph, and R. A. Buhrman, Phys. Rev. Lett. **89**, 226802 (2002).
7. W. Zaets and K. Ando, IEEE Photon. Technol. Lett. **11**, 1012 (1999).
8. V. Zayets and K. Ando, Appl. Phys. Lett. **86**, 261105 (2005).
9. T. Amemiya, H. Shimizu, Y. Nakano, P. N. Hai, M. Yokoyama, and M. Tanaka, Appl. Phys. Lett. **89**, 021104 (2006).
10. H. Shimizu and Y. Nakano, J. Lightwave Technol. **24**, 38 (2006).
11. W. Van Parys, B. Moeyersoon, D. Van Thourhout, R. Baets, M. Vanwolleghem, B. Dagens, J. Decobert, O. Le Gouezigou, D. Make, R. Vanheertum, and L. Lagae, Appl. Phys. Lett. **88**, 071115 (2006).
12. R. H. Cox and H. Strack, Solid-State Electron. **10**, 1213 (1967).
13. S. A. Crooker, M. Furis, X. Lou, C. Adelmann, D. L. Smith, C. J. Palmstrøm, and P. A. Crowell, Science **309**, 2191 (2005).
14. V. F. Motsnyi, V. I. Safarov, J. De Boeck, J. Das, W. Van Roy, E. Goovaerts, and G. Borghs, Appl. Phys. Lett. **81**, 265 (2002).
15. A. Sinsarp, T. Manago, F. Takano, and H. Akinaga, Jpn. J. Appl. Phys. Part 2 **46**, L4 (2007).
16. O. M. J. van't Erve, G. Kioseoglou, A. T. Hanbicki, C. H. Li, B. T. Jonker, R. Mallory, M. Yasar, and A. Petrou, Appl. Phys. Lett. **84**, 4334 (2004).
17. X. Jiang, R. Wang, R. M. Shelby, R. M. Macfarlane, S. R. Bank, J. S. Harris, and S. S. P. Parkin, Phys. Rev. Lett. **94**, 056601 (2005).